

The Global Structure and Evolution of a Self-Gravitating Multi-phase Interstellar Medium in a Galactic Disk

Keiichi Wada¹ and Colin Norman²

Department of Physics and Astronomy,
Johns Hopkins University, Baltimore, MD 21218

ABSTRACT

Using high resolution, two-dimensional hydrodynamical simulations, we investigate the evolution of a self-gravitating multi-phase interstellar medium in the central kiloparsec region of a galactic disk. We find that a gravitationally and thermally unstable disk evolves, in a self-stabilizing manner, into a globally quasi-stable disk that consists of cold ($T < 100$ K), dense clumps and filaments surrounded by hot ($T > 10^4$ K), diffuse medium. The quasi-stationary, filamentary structure of the cold gas is remarkable. The hot gas, characterized by low-density holes and voids, is produced by shock heating. The shocks derive their energy from differential rotation and gravitational perturbations due to the formation of cold dense clumps. In the quasi-stable phase where cold and dense clouds are formed, the effective stability parameter, Q , has a value in the range 2-5. The dynamic range of our multi-phase calculations is $10^6 - 10^7$ in both density and temperature. Phase diagrams for this turbulent medium are analyzed and discussed.

Subject headings: ISM: structure, kinematics and dynamics — galaxies: structure — method: numerical

1. INTRODUCTION

We model the multi-phase and inhomogeneous interstellar medium (ISM) in the inner region of a galactic disk including fundamental physical processes crucial for understanding star formation, global and local dynamics of the ISM in galaxies, and aspects of galaxy

¹National Astronomical Observatory, Mitaka, 181, Japan (email: wada@th.nao.ac.jp)

²Space Telescope Science Institute, Baltimore, MD 21218 (email: norman@stsci.edu)

formation such as feedback. Most numerical simulations of the ISM and of star formation in galaxies have assumed simpler ISM models, e.g. an isothermal or nearly-isothermal equation of state, and either a smooth medium or discrete clouds. There are some notable exceptions. Pioneering work by Bania & Lyon (1980), in which the effects of OB stars on the multi-phase ISM have been investigated using two-dimensional hydrodynamics using 40×40 grid cells for a $180 \text{ pc} \times 180 \text{ pc}$ region. More recently, Rosen, Bregman & Norman (1993) and Rosen & Bregman (1995) have studied dynamics of the multi-phase ISM. Their simulations are for two-fluids (gas and stars) in two-dimensions, but they ignored the self-gravity of the gas and the effect of galactic rotation. Self-gravity of the gas is necessary to produce very high density clouds which are the sites of star formation. Rotation and the associated differential shear are also important elements for the global gas dynamics and ISM structure. Vázquez-Semadeni et al. (1995) and Passot et al. (1995) have studied self-gravitating supersonic turbulence with 2-D hydrodynamic and magnetohydrodynamic simulations. They also took into account Coriolis force and large-scale shear. They assumed, however, periodic-boundaries with a local-shearing coordinate. They also introduced an artificial mass diffusion term in the continuity equation. As discussed in their paper, this term smoothes out the density gradient, and prevents the generation of large density contrasts and strong shocks. A full three-dimensional simulations of gas and stars in a galaxy has been made by Gerritsen & Icke (1997), using the SPH technique. They have a roughly two-phase structure of the ISM. Although the SPH is quite powerful for three-dimensional problems, it is hard to achieve a pc-scale resolution in 3-D for the ISM in a whole galaxy. One cannot avoid introducing *ad hoc* assumptions for star formation and its energy feedback to the ISM without a pc-scale resolution.

In this *Letter*, we report on the structure and global evolution of multi-phase ISM models in two-dimensions, taking into account self-gravity of the gas, galactic rotation, radiative cooling, and heating due to UV background radiation. The effects of heating due to stellar winds from massive stars and SNe are discussed in a subsequent paper. We use an Eulerian hydro-code without periodic boundary conditions. Our code allow us to handle over seven orders of magnitude for density and temperature in a $\sim \text{kpc}$ -scale region around the galactic center with $\sim \text{pc}$ -scale resolution.

2. NUMERICAL METHOD AND MODELS

We solve the following equations numerically in two-dimensions to simulate the evolution of a rotating disk.

$$\frac{\partial \rho}{\partial t} + \nabla \cdot (\rho \mathbf{v}) = 0, \quad (1)$$

$$\frac{\partial \mathbf{v}}{\partial t} + (\mathbf{v} \cdot \nabla) \mathbf{v} + \frac{\nabla p}{\rho} + \nabla \Phi_{\text{ext}} + \nabla \Phi_{\text{sg}} = 0, \quad (2)$$

$$\frac{\partial E}{\partial t} + \frac{1}{\rho} \nabla \cdot ((\rho E + p) \mathbf{v}) = \Gamma_{\text{UV}} - \rho \Lambda(T_g), \quad (3)$$

$$\nabla^2 \Phi_{\text{sg}} = 4\pi G \rho, \quad (4)$$

where, ρ, p, \mathbf{v} are the density, pressure, and velocity of the gas, and the specific total energy $E \equiv |\mathbf{v}|^2/2 + p/(\gamma - 1)\rho$, with $\gamma = 1.4$. We assume a time-independent external potential $\Phi_{\text{ext}} \equiv -(27/4)^{1/2} v_c^2 / (R^2 + a^2)^{1/2}$, where a is a core radius of the potential and v_c is the maximum rotational velocity. We also assume a cooling function $\Lambda(T_g)$ ($10 < T_g < 10^8 \text{K}$) (Spaans & Norman 1997) and a heating function Γ_{UV} .¹ We assume a uniform UV radiation field, which is normalized to the local interstellar value, and photoelectric heating of grains and PAHs.

The hydrodynamic part of the basic equations is solved by AUSM (Advection Upstream Splitting Method) (Liou & Steffen 1993) with a van Leer-type flux splitting process (Liou 1996). After testing this code for various hydrodynamical 1-D and 2-D problems, we find that AUSM is as powerful a scheme for astrophysical problems as are the PPM (Woodward & Colella 1984) and Zeus (Stone & Norman 1992) codes. We achieve third-order spatial accuracy with MUSCL (van Leer 1977). To satisfy the TVD condition using MUSCL, we use the minmod limiting function. More details about our numerical code and test results are described in Wada & Norman (1998, in preparation).

We use 1024^2 Cartesian grid points covering a $2 \text{ kpc} \times 2 \text{ kpc}$ region. Therefore, the spatial resolution is 1.95 pc with 2048^2 grid cells. A periodic Green function is used to calculate the self-gravity for the 1024^2 grid points (Hockney & Eastwood 1981). The second-order leap-frog method is used for the time integration. We adopt implicit time integration for the cooling term.

The initial condition are an axisymmetric and rotationally supported disk with the Toomre stability parameter $Q = 1.2$ over the whole disk. Random density and temperature fluctuations are added to the initial disk. These fluctuations are less than 1 % of the

¹ In previous simulations on the multi-phase ISM, the minimum temperature was assumed as 300 K (Rosen, Bregman, & Norman 1993; Rosen & Bregman 1995; Vázquez-Semadeni et al. 1995; Passot et al. 1995) or 100 K (Vázquez-Semadeni et al. 1996).

unperturbed values and have an approximately white noise distribution. The initial temperature is set to 10^4 K over the whole region. In ghost zones at the boundaries, all physical quantities remain at their initial values during the calculations. From test runs we found that these boundary conditions are much better than ‘outflow’ boundaries, because the latter cause strong unphysical reflection of waves at the boundaries.

3. RESULTS

3.1. Morphology and Evolution

Figure 1 shows the density and temperature distribution of the central $2 \text{ kpc} \times 2 \text{ kpc}$ region at $t = 166 \text{ Myr}$. The structure is quasi-stable after $t \sim 50 \text{ Myr}$. The density range is from 10^{-1} to $10^6 M_\odot \text{ pc}^{-2}$, which corresponds to about 0.03 to $3 \times 10^5 \text{ cm}^{-3}$. The most prominent feature of the resulting quasi-stable structure is its filamentary appearance. The high density clumps are embedded in less dense filaments ($\Sigma_g \sim 10^{3-4} M_\odot \text{ pc}^{-2}$ and $T_g \lesssim 100 \text{ K}$). The characteristic size of the highest density clouds ($\Sigma_g \geq 10^5 M_\odot \text{ pc}^{-2}$) is about 5-50 pc. It is notable that the density and temperature structures are well correlated: high temperature gas corresponds to low density gas, and low temperature gas corresponds to high density gas. This means that the thermal structure in this system is driven by the density, because the radiative cooling is very effective. The temperature of the very low density gas in the voids sometimes reaches 10^6 K , due to shock heating. The energy source of this heating is the turbulent, random motion of the gas, at velocities $\sim 100 \text{ km s}^{-1}$. The maximum vorticity is $\sim 40 \text{ km s}^{-1} \text{ pc}^{-1}$. There are strong local shear motions associated with the filaments.

Figure 2 is a phase diagram ($p_{\text{th}} \equiv \Sigma_g T_g$ vs. Σ_g) for the model shown in Fig.1. The left and right diagonal lines correspond to states in which the gas temperature is 10^4 and 10 K . There are also two less prominent ‘ridges’ between the hot and cold phases, i.e. $(p_{\text{th}}, \Sigma_g) = (3, 1) - (2.5, 2)$ and $(2.5, 2) - (4, 4)$. One ridge corresponds to filaments with temperature, $T_g \sim 200 \text{ K}$. The second ridge indicated by a dotted line has ‘negative γ ’ where γ is the adiabatic index. The gas in this state is thermally unstable. In spite of this instability the gas component does not have temporal variations. This is not a paradox, if we consider the kinematic or turbulent pressure of the gas as well as the thermal pressure. As can be seen in this phase diagram, the system cannot be described as a simple two- or three-phase media with pressure equilibrium between the phases.

Although the initial Q value is 1.2 (i.e. the disk is stable for an axisymmetric modes), the effective Q value becomes much less than unity after a few Myr (see §3.2 and Fig.3),

because the cooling time is very short. The gas temperature decreases from the initial value ($\sim 10^4$ K) to an equilibrium temperature ($\sim 10^2$ K) within 10^5 yr. Since the initial density is higher in the central region of the disk than in the outer region, gravitational instabilities begin in the inner few 100 pc and develop outward. At $t \sim 10$ Myr (\sim one rotational period at $R \sim 200$ pc), the gravitational instabilities in the central 500 pc are already in a non-linear phase, where the maximum density contrast is about 10^6 . At $t \sim 25$ Myr, the instability grows non-linearly over the whole disk, and many clumps, filaments and low density voids are formed. The outer region of this multi-phase disk expands until, at about $t = 50$ Myr, it reaches a quasi-stable state. The total entropy of the system increases very rapidly in the first 20 Myr, and it remains roughly constant after 30 Myr. The entropy generation by shocks is balanced by radiative cooling to maintain this stationary state.

About 80 % of the mass is in the cold ($T_g < 100$ K) phase. In other words, the cold, dense clumps dominate the total gas mass. The second most dominant phase is the warm ($100 < T_g < 9000$ K) gas. The mass of this warm gas increases from $10^7 M_\odot$ to $10^8 M_\odot$ in the first 10 Myr. It is notable that the gas mass in the hot phase ($T_g > 10^4$ K) increases by a factor of order $\sim 10^2$ for the first 30 Myr. In the quasi-stable phase, the hot gas occupies about 0.3% of the total mass. As expected, on the other hand, the volume filling factors of the hot, warm and cold gas indicate that the hot gas ($T_g \geq 9000$ K) occupies a volume $10^{2.5}$ times larger than the cold gas. The volume filling factor for the gas in the temperature range $11000 \leq T_g < 10^5$ K increases from 0 to 30% until $t = 30$ Myr. In contrast, the cold gas fraction decreases from 48% to 10% in the same period. After 30 Myr, the volume filling factor of each component does not change appreciably, and this also shows that the system reaches a quasi- equilibrium state.

The radial mass distribution has roughly exponential shape after 50 Myr, and the profile at 165 Myr becomes a steeper exponential. The density inside $R = 100$ pc becomes about 4 times larger at $t = 165$ Myr. The total gas mass inside this region is about $3 \times 10^7 M_\odot$, which is comparable to the dynamical mass. The evolution of the radial profile implies outward transport of angular momentum. In fact, 5 % of total specific angular momentum is transferred through the outer boundary. This is due to random motion of the flow caused by the non-linear evolution of the gravitational instability. Although the global density profile is exponential, it fluctuates by a factor of ~ 2 -3 in over scales of order ~ 100 pc. These fluctuations correspond to complexes of clouds and filaments that form weak spiral-like patterns as seen in Fig.1.

3.2. Self-stabilization due to Dynamical Heating

The evolution of Toomre’s Q parameter in this system is very interesting, because this parameter has been often supposed to be a good criterion for star formation in disk galaxies (e.g. Kennicutt 1989). Figure 3 shows a radial distribution of an effective Q value (Q_{eff}) at $t = 10, 25, 50, 166$ Myr of a model without star formation. Q_{eff} is defined as $Q_{\text{eff}}(R) \equiv \kappa \sigma_v / \pi G \Sigma_g$, where κ is the epicyclic frequency. The azimuthally averaged ($\Delta R = 20$ pc) velocity dispersion σ_v is defined by $\sigma_v \equiv \sqrt{\langle v^2 \rangle_{\Delta R} - \langle v \rangle_{\Delta R}^2}$ with $v \equiv |\mathbf{v}| + c_s$, where \mathbf{v} the flow velocity and c_s is the sound velocity of the gas. As mentioned above, the initial Q_{eff} becomes far less than unity almost everywhere in the disk after 1 Myr. However, after 50 Myrs, Q_{eff} increases above the marginal stability value for the whole disk. This means that the system is globally self-stabilized. We found that the stabilization is mostly due to the increase of the velocity dispersion of the gas, rather than large sound velocity in the high temperature gas arising from the shock heating. The averaged velocity dispersion increases to $\sim 15\text{-}20$ km s $^{-1}$ in 50 Myr, whereas the averaged sound speed increases from about 3 km s $^{-1}$ to 8 km s $^{-1}$.²

The multi-phase disk is *locally* unstable, however it is *globally* stable, as shown by Q_{eff} . This suggests that the Toomre’s Q might not be useful directly here as a star formation criterion, because there are many cold and dense clumps formed even at effective values of Q significantly greater than unity. In such cold and dense clumps, the Jeans length is much smaller than the characteristic size of the clumps. Therefore, we expect star formation in the clumps. Energy feedback from such stars to the ISM, the ultimate fate of the dense clouds and the global structure of the multi-phase ISM are interesting problems and are discussed in subsequent papers.

It is notable that the multi-phase, quasi-stable ISM is formed from a highly gravitationally and thermally unstable state without heating due to SNe. The diffuse UV heating does not contribute to the global stabilization. Shock heating is a dominant heating mechanism for $T_g > 10^4$ K in this system. Shearing of the disk induced by differential rotation and gravitational perturbation from clumps are the main energy source for the shock heating.

²It is of interest to compare this velocity dispersion with the internal velocity dispersion of GMCs to understand the mechanism that maintains the internal motion of GMCs. Although the dispersion, $\sim 15\text{-}20$ km s $^{-1}$, is in the same order of the observed line width for GMCs in the central region of our Galaxy, our spatial resolution (~ 2 pc) is still insufficient for a detailed comparison with the internal motion of GMCs.

4. SUMMARY AND DISCUSSIONS

We have shown that a globally stable, multi-phase ISM is formed as a natural consequence of the non-linear evolution of a self-gravitating gas disk. The gas is in so many and such various phases represented by a wide range of density and temperature that multi-phase is probably an inadequate description. The gas has properties more like a phase continuum. The density ranges over seven orders of magnitude from $10^{-1} - 10^6 M_{\odot} \text{ pc}^{-2}$, and the temperature extends from $10 - 10^8$ K. We found that the ISM cannot be expressed simply by the two-phase or three-phase model (e.g. McKee & Ostriker 1977; Ikeuchi, Habe, & Tanaka 1984; Norman & Ikeuchi 1989; Norman & Ferrara 1996), because the gas dynamic processes, such as turbulence, global rotation, shear motion and shocks, are at least as important as thermal processes. Our high resolution Eulerian hydrodynamic code allows us to handle gas dynamics on a kiloparsec scale with a few parsec resolution regardless of the gas density. Possible star forming sites where the gas density is very high ($n \gtrsim 10^4 \text{ cm}^{-3}$) and the temperature is less than 100 K can be identified clearly. The evolution of supernova remnants in an inhomogeneous and rotating media is fully followed as discussed in a subsequent paper. The multi-phase structure of the gas is very complicated, and is characterized by filamentary and clumpy substructure as well as low density holes and voids surrounded by the denser media.

Although our numerical simulations show the potential of more realistic models of the ISM and of star formation than in previous simulations with lower resolution, there are a number of physical aspects of the real ISM that should be considered in future models: the ionization state of the gas; the non-uniform UV radiation field due to massive stars; magnetic fields; the chemical evolution and dynamics of the stellar component and its interaction with the gaseous component. Besides these physical processes, three-dimensional simulations need to be considered. Our numerical scheme can be extended to three-dimensions, and in fact such simulations are currently possible but at the expense of either resolution or dynamic range in the disk.

Our results show that the description of the ISM can be moved to a more realistic level using techniques such as we have discussed here. This has interesting implications for many aspect of galaxies. In particular, we should now consider the complex nature and dynamics of the multi-phase and inhomogeneous ISM in theories of star formation, galaxy formation and galaxy evolution.

We would like to thank the referee, V. Icke, and T. Hasegawa for their helpful suggestions. We are grateful to M. Spaans for providing us the cooling functions and stimulating and useful discussions. We thank D. Strickland for his fruitful comments on

the draft. We also acknowledge stimulating discussions with the members of the *HOT TOPICS* group at JHU. KW thanks Yamada Science Foundation for their support at STScI. Numerical computations were carried out on VPP300/16R at the Astronomical Data Analysis Center of the National Astronomical Observatory, Japan. This work has been supported in part by NASA Grant NAG8-1133.

REFERENCES

- Bania, T. M. & Lyon, J. G., 1980, ApJ, 239, 173
- Gerritsen, J. P. E., Icke, V., 1997, A&Ap, 325, 972
- Hockney, R. W., Eastwood, J. W. 1981, Computer Simulation Using Particles (New York : McGraw Hill)
- Ikeuchi, S., Habe, A., Tanaka, Y. D., 1984, MNRAS, 207, 909
- Kennicutt, R., 1989, ApJ, 344, 685
- Liou, M., Steffen, C., 1993, J.Comp.Phys., 107,23
- Liou, M., 1996, J.Comp.Phys., 129,364
- McKee, C.F. & Ostriker, J.P. 1977, ApJ, 218,148
- Norman, C.A., & Ikeuchi, S., 1989, ApJ, 345,372
- Norman, C.A., & Ferrara, A., 1996, ApJ, 467, 280
- Passot, T., Vázquez-Semadeni, E., & Pouquet, A. 1995, ApJ, 455, 536
- Rosen, A., Bregman, J.N., 1995,ApJ, 440, 634
- Rosen, A., Bregman, J.N., Norman, M.L. 1993,ApJ, 413, 137
- Spaans, M., Norman C., 1997, ApJ, 483, 87
- Stone, J., Norman, M.N. 1992, APJS, 80, 753
- van Leer, B., 1977, J.Comp.Phys., 32, 101
- Vázquez-Semadeni, E., Pasot, T. & Pouquet, A. 1995, ApJ, 441, 702
- Vázquez-Semadeni, E., Pasot, T. & Pouquet, A. 1996, ApJ, 473, 881
- Woodward, P. R., Colella, P. 1984, J.Comp.Phys., 54, 115

Fig. 1.— Density (left) and temperature (right) map at $t = 166$ Myr. The color bar is log-scale. The density range is 10^{-1} to $10^5 M_{\odot} \text{ pc}^{-2}$, and temperature range is $10 - 10^8$ K.

Fig. 2.— Pressure ($\Sigma_g T_g$) vs. density (Σ_g) phase diagram for the model shown in Fig. 1. Three diagonal lines show the gaseous temperature 10^4 K, 190 K, and 10 K. The dotted line means thermally unstable gas.

Fig. 3.— Evolution of the effective Toomre Q as a function of radius. Thin line with +, dashed line, dotted line, and solid line are for $t = 10, 25, 50, 166$ Myr respectively. $Q_{\text{eff}} < 1$ means the system is unstable.

This figure "Fig1.gif" is available in "gif" format from:

<http://arxiv.org/ps/astro-ph/9903171v1>

Fig. 2

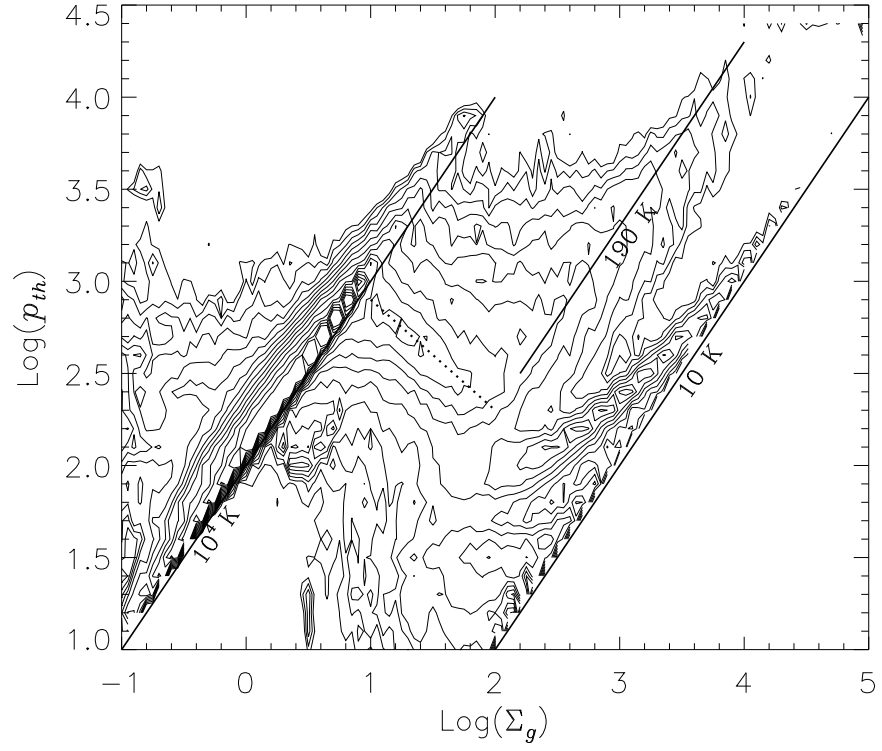


Fig.3

